# SYNTHESIS AND CHARACTERIZATION OF LOW BANDGAP NANOCRYSTALLINE t-ZIRCONIA

**NIKI PRASTOMO**

**UNIVERSITI SAINS MALAYSIA**

**2007**

Saya isytiharkan bahawa kandungan yang dibentangkan di dalam tesis ini adalah hasil kerja saya sendiri dan telah dijalankan di Universiti Sains Malaysia kecuali dimaklumkan sebaliknya. Tesis ini juga tidak pernah disertakan untuk ijazah yang lain sebelum ini.

Disaksikan Oleh:

.....  .....

Tandatangan Calon  Tandatangan Penyelia/Dekan

Nama Calon: Niki Prastomo

# SYNTHESIS AND CHARACTERIZATION OF LOW BANDGAP NANOCRYSTALLINE t-ZIRCONIA

**by**

NIKI PRASTOMO

**Thesis submitted in fulfillment of the requirements
for the degree of
Master of Science**

**July 2007**

## ACKNOWLEDGEMENTS

I cherish this chance to show my sincere gratefulness to my supervisors Assoc. Prof. Dr. Ahmad Fauzi Mohd Noor and Dr Zainovia Lockman for their constant support, encouragement, knowledge and valuables guidance during research project at Materials Engineering, School of Materials & Minerals Resources Engineering, Universiti Sains Malaysia. Inspired by them, I learned the true spirit of being a scientist. I believe that hard work and consistent devotion are the keys to success. They have become wonderful mentors for my work and my life. Then I would like to acknowledge my advisor, Prof. Atsunori Matsuda at Department of Materials Science, Faculty of Engineering, Toyohashi University of Technology, for his valuables comment and input throughout the project. I wish to thank my advisor, Dr. Ahmad Nuruddin in ITB, for his support and suggestions. I also would like to express my gratitude to Prof. P. Pramanik of Department of Chemistry Indian Institute of Technology for supporting this work.

I would like to thank Dean, Assoc. Prof. Dr. Khairun Azizi Mohd. Azizli and to all the members, past and present, of the Materials Engineering Study Program for their kind assistance and supports, all the technical staffs, especially Mr. Sahrul, Ms Fong, Mrs. Haslina, Mr. Hasnur, Mr. Helmi, Mr. Farid, Mr. Rashid, Mr. Azam, Mr. Mokhtar, and Mr. Shahid for their invaluable assistance and technical support.

I am grateful to JICA-AUN/SEED-Net program for financial support and the opportunity to undertake this work. Thank you very much to AUN/SEED-Net Chief Advisor, Prof. Dr. Kazuo Tsutsumi, Mr. Sakae Yamada, Ms. Kalayaporn, Ms. Meena, Ms Rungchalai, Ms. Irda, and Ms. Norpisah.

I want to thank all my group members including Koay Seong Tak, Wong Gar Shen, Siew Fook Wai, Ch'ng Lay Ean, Nur Azila, Roshasnorlyza, Sam Sung Ting, Aye

Aye Thant, Umar Al-amani, Firmandika Harda and Dr. Teoh Wah Tzu for their valuable assistance. Without their technical support and friendship, I could not have possibly finished my study here easily.

I want to express gratitude to all postgraduate students in School of Materials & Mineral Resources Engineering USM, it was an unforgettable moment having great companion during my study. All activities that we had together will be etched in my mind.

Thanks to all my friends in PPI's Engineering, especially for B'Sobron, Hosta, Asep, B'Irvan, P'Teguh, B'Heri, P'Kusmono, K'Hamidah, B'zul, B'Fatur, B'Irtan and Mba Yanti for their support and friendship. Finally, I would like to take this opportunity to express my gratitude to my family members for their love, unfailing encouragement and support, specially my parents. Special thanks to my dear Winda Deftiani Putri for her endless care, encouragement and support.

## TABLE OF CONTENTS

## CHAPTER 3 : MATERIALS AND METHODOLOGY

## CHAPTER 4 : RESULTS AND DISCUSSION

## LIST OF TABLES

## LIST OF FIGURES

## LIST OF ABBREVIATION

| | | |
|---|---|---|
| Ca | : | Calcium |
| Ce | : | Cerium |
| Cu | : | Copper |
| CB | : | Conduction Band |
| c-$ZrO_2$ | : | Cubic Zirconia |
| BET | : | Surface Area Measurements |
| DTA | : | Differential Thermal Analysis |
| $E_F$ | : | Fermi Energy |
| $E_g$ | : | Bandgap Energy |
| FESEM | : | Field Emission Scanning Electron Microscope |
| FSZ | : | Fully Stabilized Zirconia |
| GaN | : | Gallium Nitride |
| ICDD | : | International Centre for Diffraction Data |
| JCPDS | : | Joint Committee on Powder Diffraction Standards |
| LTD | : | Low Temperature Degradation |
| MSDS | : | Materials Safety Data Sheet |
| m-$ZrO_2$ | : | Monoclinic Zirconia |
| Mg | : | Magnesium |
| Nb | : | Niobium |
| NHE | | Normal Hydrogen Electron |
| nm | : | nano meter |
| PSZ | : | Partially Stabilized Zirconia |
| SEM | : | Scanning Electron Microscope |
| SiC | : | Silicon Carbide |
| SOFC | : | Solid Oxide Fuel Cells |
| SPG | : | Secondary Precipitate Growth |
| TEA | : | Tri Ethanol Amine |
| TEM | : | Transmission Electron Microscope |
| TG | : | Thermo Gravimetry |
| Th | : | Thorium |
| Ti | : | Titanium |
| $TiO_2$ | : | Titanium Oxide |
| TZP | : | Tetragonal Zirconia Polycrystalline |

| | | |
|---|---|---|
| t-$ZrO_2$ | : | Tetragonal ZIrconia |
| UV | : | Ultra Violet |
| VB | : | Valence Band |
| $YNbO_4$ | : | Yttrium Niobium Oxide |
| XRD | : | X-Ray Diffraction |
| Y | : | Yttrium |
| YSZ | : | Yttria Stabilized Zirconia |
| Zr | : | Zirconium |
| $ZrO_2$ | : | Zirconia |
| ZTM | : | Zirconia Toughened Mullite |

## LIST OF SYMBOLS

| | | |
|---|---|---|
| $a_c$ | : | "a" axis value of cubic phase (Å) |
| $a_m$ | : | "a" axis value of monoclinic phase (Å) |
| $a_t$ | : | "a" axis value of tetragonal phase (Å) |
| A | : | Specific Surface Area ($g/m^2$) |
| $b_m$ | : | "b" axis value of monoclinic phase (Å) |
| $\beta$ | : | angle between "a" and "c" axes (°) |
| $c_m$ | : | "c" axis value of monoclinic phase (Å) |
| $c_t$ | : | "c" axis value of tetragonal phase (Å) |
| $d_{hkl}$ | : | Interplanar Spacing (Å) |
| e | : | Electron |
| hkl | : | Miller Indices |
| hv | : | Photon Energy (eV) |
| $I_c$ | : | X-Ray intensity of cubic phase |
| $I_m$ | : | X-Ray intensity of monoclinic phase |
| $I_t$ | : | X-Ray intensity of tetragonal phase |
| $\lambda$ | : | wavelength of the X-Ray radiation (nm) |
| $\rho$ | : | Density ($g/cm^3$) |
| V | : | Volume pellets ($cm^3$) |
| $v_c$ | : | Volume fraction of cubic phase (%) |
| $v_m$ | : | Volume fraction of monoclinic phase (%) |
| $V_{\ddot{O}}$ | : | Oxygen Vacancy |
| $v_t$ | : | Volume fraction of tetragonal phase (%) |
| $\theta$ | : | Angle (°) |

## LIST OF PUBLICATIONS

1. Niki Prastomo, Zainovia Lockman, Ahmad Nuruddin, Atsunori Matsuda, Ahmad Fauzi Mohd Noor. (2006) Preliminary Study On Chemical Synthesis Of Nanocrystals Semi-Conducting Tetragonal Zirconia. *Proceeding 3rd School of Materials and Mineral Resources Engineering USM Postgraduate Research Paper*, Published by SMMRE, USM, Pulau Penang, Malaysia. 2005/2006, p58

2. Niki Prastomo, Zainovia Lockman, Ahmad Nuruddin, Atsunori Matsuda, Ahmad Fauzi Mohd Noor. (2006) Chemical Synthesis Of Nanocrystals Semi-Conducting Tetragonal Zirconia Powders. *Proceeding. AUN/SEED-Net/JICA Field-Wise Seminar VIII*, 22nd-23rd May 2006, Pulau Pinang, published by School of Materials and Mineral Resources Engineering, Universiti Sains Malaysia, 14300 Nibong Tebal, Pulau Pinang, Malaysia.

3. Niki Prastomo, Zainovia Lockman, Ahmad Nuruddin, Atsunori Matsuda, Ahmad Fauzi Mohd Noor. (2006) Chemical Synthesis Of Nanocrystals Tetragonal Zirconia Powders. *Proceeding. Nano MIG Seminar*, 22nd June 2006, School of Materials and Mineral Resources Engineering, Universiti Sains Malaysia, 14300 Nibong Tebal, Pulau Pinang, Malaysia.

4. Niki Prastomo, Zainovia Lockman, Ahmad Nuruddin, Atsunori Matsuda, Ahmad Fauzi Mohd Noor. (2006) Soft Combustion Synthesis Of Nanocrystalssemi-Conducting Tetragonal Zirconia Powders. *Proceeding. Asian Symposium on Materials and Processing (ASMP) 2006*, 9th -10th November 2006. The Japan Society of Mechanical Engineers, Bangkok, Thailand.

5. Niki Prastomo, Zainovia Lockman, Ahmad Nuruddin, Atsunori Matsuda, Panchanan Pramanik, Ahmad Fauzi Mohd Noor. (2006) Soft Combustion Synthesis Of Nanocrystalssemi-Conducting Tetragonal Zirconia Powders. *Proceeding. International Conference on X-Rays and Related Techniques in Research and Industry (ICXRI) 2006*, 29th-30th November 2006. Malaysian Institute for Nuclear Technology Research, Putrajaya, Kuala Lumpur, Malaysia.

6. Niki Prastomo, Zainovia Lockman, Ahmad Nuruddin, Atsunori Matsuda, Ahmad Fauzi Mohd Noor. (2007) The Effect Of Nb-Doping On Tetragonal Y-Zirconia. *Proceeding. International Conference on Engineering and Environment (ICEE) 2007*. 10th-11th May 2007. Faculty of Engineering, Prince of Songkla University, Thailand.

## SINTESIS DAN PENCIRIAN t-ZIRKONIA NANOHABLUR DENGAN SELA JALUR RENDAH

## ABSTRAK

Serbuk nanohablur t-$ZrO_2$ disintesis melalui kaedah kimia untuk mencari kemungkinan jika dop elektronik akan meningkatkan konduktiviti elektronik oksida. $Y^{3+}$ ditambah sebagai penstabil untuk mengekalkan fasa t-$ZrO_2$ manakala $Nb^{5+}$ dimasukkan untuk dop elektronik. Fasa pembentukan dan penstabilan untuk memperolehi 100% t-$ZrO_2$ dikaji secara terperinci dengan menggunakan kesemua parameter yang mempunyai kemungkinan untuk menyumbang fasa pembentukannya. Melalui kajian ini, dop zirkonia disediakan melalui kaedah penguraian polimer dan kaedah pembakaran lembut. Untuk kaedah penguraian polimer, larutan mediumnya disediakan daripada campuran zirkonil nitrat ($ZrO(NO_3)_2$), yttrium nitrat ($Y(NO_3)_3$), niobium tartarat ($HNb(C_4O_6)$) dan TEA (triethanolamine) manakala untuk kaedah pembakran lembut, hanya zirkonil nitrat, yttrium nitrat, niobium nitrat ($Nb(NO_3)_5$) dan glisin digunakan. Beberapa komposisi dop serbuk zirkonia telah disediakan melalui kaedah penguraian terma pada suhu yang berbeza. Serbuk yang dihasilkan telah dicirikan dengan menggunakan Analisis Perbezaan Terma (DTA), Pembelauan Sinar-X (XRD), Pengimbas Mikroskopi Elektron (SEM) dan Penghantaran Mikroskopi Elektron (TEM). Purata saiz partikel kalsin pada 700°C dalam kajian ini adalah dalam lingkungan 13 sehingga 38 nm. Penambahan $Nb^{5+}$ tidak mengubah kestabilan sintesis serbuk dalam fasa tetragonal. Apabila disinter dalam atmosfera yang berlainan (argon-karbon, vakum dan udara) didapati pensinteran pada suhu yang tinggi menyebabkan t-$ZrO_2$ berubah ke m-$ZrO_2$. Walau bagaimanapun 100% t-$ZrO_2$ dikekal dengan pensinteran pada suhu 1400°C dalam atmosfera vakum. Sela jalur optik dikira menggunakan Spektrometer Ultra Ungu-Cahaya Nampak keatas sample sinter dengan t-$ZrO_2$ memberikan nilai minima 4.00 eV, lebih rendah daripada sela jalur Zirkonia Terstabil Yttria (YSZ) komersil dengan nilai 6.09 eV.

# SYNTHESIS AND CHARACTERIZATION OF LOW BANDGAP NANOCRYSTALLINE t-ZIRCONIA

## ABSTRACT

Nanocrystal t-$ZrO_2$ powders were synthesized through a chemical route to seek a possibility if electronic doping would improve the electronics conductivity of the oxide. $Y^{3+}$ was added as a stabilizer to retain tetragonal phase $ZrO_2$ whereas $Nb^{5+}$ was added for electronics doping. The phase formation and stabilization to achieve 100% pure t-$ZrO_2$ were studied in detail encompassing all possible parameters which would contribute to the phase formation. Polymer decomposition and soft combustion methods were performed in this study to produce the doped zirconia. Precursor solutions were prepared from a mixture of zirconyl nitrate ($ZrO(NO_3)_2$), yttrium nitrate ($Y(NO_3)_3$), niobium tartarate ($HNb(C_4O_6)$) and TEA (triethanolamine) for polymer decomposition method, while zirconyl nitrate, yttrium nitrate, niobium nitrate ($Nb(NO_3)_5$) and glycine were used in soft combustion method. Several dopants compositions of zirconia powders were prepared by thermal decomposition method and were annealed at different temperatures. The synthesized powders were characterized using Differential Thermal Analysis (DTA), X-ray Diffraction (XRD), Scanning Electron Microscopy (SEM) and Transmission Electron Microscopy (TEM). The average particle size of the powders calcined at 700ºC in this study ranges from 13.00 to 38.00 nm. The addition of $Nb^{5+}$ did not alter the stability of the tetragonal phase formed in powder synthesis. Upon sintering different kind of atmosphere (argon-carbon, vacuum and air) it was found that at high sintering temperature, 1250°C to 1600°C, t-$ZrO_2$ had transformed to m-$ZrO_2$. However 100% t-$ZrO_2$ was retained with sintering at 1400°C in vacuum condition. The optical band gap as measured by the UV-Visible Spectrometer for the sintered sample with t-$ZrO_2$ gave a minimum value 4.00 eV, lower than the optical bandgap from commercial Yttria Stabilized Zirconia (YSZ) which was 6.09 eV.

# CHAPTER 1
# INTRODUCTION

## 1.1 Background and Problem Statement

As a result of continuous research and development, zirconia ($ZrO_2$) has been used in many wear resistant and refractory applications such as piston caps, extrusion dies and machinery wear parts, as well as a solid electrolyte in furnace elements, fuel cells and oxygen sensors [Amelinck et al., 1997]. The important role of $ZrO_2$ in industrial application is attributed to its good physical properties such as high flexural strength (~1 GPa), good fracture toughness (~10 MPa $m^{1/2}$), high temperature stability and optimal dielectric constant ($\varepsilon_0$) of around 20 [Munoz et al., 2006].

Below ~1170ºC zirconia occur in the monoclinic crystal structure (m-$ZrO_2$), while between ~1170ºC-2370ºC zirconia has a tetragonal crystal structure (t-$ZrO_2$). Above 2370ºC to the melting point at 2680ºC, zirconia is in cubic structure (c-$ZrO_2$). However, metastable t-$ZrO_2$ often appears at room temperature besides m-$ZrO_2$, and by doping with low amount of metal oxides as well as controlled heat treatment, t-$ZrO_2$ can be retained at room temperature [Stefanc et al., 1999-a].

Many studies on the stabilization at room temperature of this high temperature phase (t and c) have been carried out by using higher size dopant of metallic oxides such as calcia [Saha and Pramanik, 1995], magnesia [Porter and Heur, 1997] and yttria [Ray et al., 2000], or lower size dopants such as tantalum [Ray et al., 2002] and niobia [Ray et al., 2003]. Study on the stabilization of ziconia using two kinds of dopants that has lower and higher size than zirconium has also been conducted [Raghavan et al., 2001]. However there are still more to be explored especially on the

electronic conductivity of the $ZrO_2$ when compositions of dopants with lower and higher size than $ZrO_2$ are added.

Lately in the last decade, studies on nanosized zirconia has gained some recognition. Various chemical methods have been used for the production of nanocrystalline zirconia-based powders, such as polymer decomposition process [Ray et al., 2001], co-precipitation [Yashima et al., 1996], sol-gel [Martinez et al., 2005] and soft combustion process [Juarez et al., 2000]. Among these processes, polymer decomposition and soft combustion methods show some advantages such as its low calcination temperature, relatively low cost compared to alkoxide-based sol-gel methods and better control of stoichiometry in comparison with co-precipitation ones, while producing powders in the nanometer range. Phase formation and stabilization for achieving 100% pure tetragonal zirconia were studied in this current work which encompasses some parameters contributing to the phase formation.

Sintering in high temperature was important to density doped t-$ZrO_2$. However, one major problem faced in sintering of $ZrO_2$ was the phase transformation from tetragonal to monoclinic [Capel et al., 2002]. Upon sintering at high temperatures more energy would be required to overcome the stabilization energy from the metal ions. Higher atomic-bonding vibration energy that could occur at high temperature breaks apart the oxygen-metal ions bonding resulting the atomic reorientation, hence leading to the phase transformation. This could induce the monoclinic formation upon cooling.

Zirconia is typically classified as an electrical insulator. Due to the significant ionic characteristic of the chemical bond between metallic cations and oxide ions, hence metallic oxides posses large band gaps [Robertson, 2004]. Their ionic nature simultaneously suppresses the formation of easily ionized shallow donors or acceptors, enhancing localization of either holes or electrons. A large energy is thus required to

delocalize these carriers. Zirconia is characterized by a roughly 5.8 eV bandgap, higher than most common semiconducting oxides like $TiO_2$ (3.5 eV) and $Ta_2O_5$ (4.4 eV) [Robertson, 2004]. The conduction band edge for zirconia is however in the range of -1.5 vs. Normal Hydrogen Electron (NHE) and the valance band is therefore +4.3 vs. NHE. Such values are adequate for photocatalytic activity of this oxide. In fact, having larger bandgap will allow absorption of light in the blue and ultraviolet region enhancing the photcatalytic activity of the oxide. Indeed, zirconia has already being used to oxidize various organic compounds forming a more benign compound safe for disposable [Robertson, 2004].

The difference between an insulator and a semiconductor is essentially only qualitative in nature; namely, insulators need to be heated to very high temperatures to acquire appreciable thermally enhanced conductivity, whereas semiconductors are the nonmetal solids which posses a noticeable electrical conductivity at room temperature [Berger, 1997].

The development of semiconductor started, in the 1870s, when the selenium photoconductivity was discovered [Berger, 1997], leading to the use of selenium in the devices for the visual image transport by telegraph. The first solid-state rectifiers of the alternating current based on selenium were made by Firtts (1883). His work was then developed by Grondahl and Geiger (1927) by using cuprous oxide. The development was followed by the useful of silicon and galenite in the electromagnetic wave detectors for radio receivers [Bose, 1904]. In the search for materials with improved parameters, the methods of material purification and single crystal growth were developed, and the properties of semiconductor materials and devices became a subject of a large number of researches, especially in silicon, germanium and transistor invention [Shockley, 1950].

The development was followed by the investigation of the electrical properties of large number of binary compounds with components that belong to the groups of periodic table equidistant from group IV. These compounds belong to one of three types, III-V, II-VI, or I-VII, with crystal structure similar to either one of the cubic mineral, sphalerite, or to hexagonal wurtzite [Berger, 1997]. Investigation of properties of the III-V and II-VI compounds shows a very successful application in semiconductor devices, such as fectifoiers, photodiodes and Gunn diodes [Gunn, 1963].

Currently, electronic materials require wide bandgaps within the range 3 to 4 eV for high voltage and temperature operation, with good transport properties. Traditional silicon based technology cannot support such requirements, but research in Gallium Nitride (GaN) [Pearton et al., 2001] and Silicon Carbide (SiC) [Burk et al., 1999] made this type of material capable of reaching similar performance level. Zirconia also has a possibility to carry out this kind of applications at high voltage and high temperature due to its high temperature stability and high toughness. However, further study on its electronic conductivity should be conducted to produce lower bandgap zirconia.

With this background, this study was embarked to investigate the possibility of zirconia as a semiconductor material. The production process of zirconia and the electronic properties via doping the oxide with yttrium ($Y^{3+}$) and niobium ($Nb^{5+}$) was explored. With its high solubility in zirconia system, $Y^{3+}$ was used to induce and stabilize t-$ZrO_2$ phase while with its high electronic conductivity, $Nb^{5+}$ was used as electronic dopant to the pure t-$ZrO_2$. As reported by Munoz et al. (2006) and Botta et al. (1999) the bandgap of t-$ZrO_2$ is in the range of 3 eV and hence pure t-$ZrO_2$ is of interest in this work due to the low bandgap value. Therefore, in this study, work was done to optimize the formation of pure tetragonal phase, with intention to lower the bandgap of zirconia by $Nb^{5+}$ doping into wide bandgap semiconductor range. It is of interest to explore this matter and evaluate if indeed t-phase of Nb-Y-$ZrO_2$ can be used

as a semiconducting materials. One possible application of this oxide would be in high power and high temperature devices, which include sensors and switches in automobile.

## 1.2 Objective of the Research

The main objective of this research work is to produce nanocrystal t-$ZrO_2$ with semiconducting properties. With this main objective, the following studies were conducted:

1 Synthesis of nanocrystal t-$ZrO_2$ powders via wet chemical process, polymeric precursor decomposition and soft combustion method.

2 Sintering of dense t-$ZrO_2$ with optimum physical properties with low bandgap value.

3 Investigation of the effect of $Nb^{5+}$ to $Y^{3+}$ ratio to the phase of $ZrO_2$ (i.e. if the tetragonal phase retained) and the bandgap value.

## 1.3 Project Overview

In this study, a wet chemical process by polymer precursor decomposition (Experiment A) and a soft combustion method (Experiment B) was selected to produce the t-$ZrO_2$. Various parameters were investigated in synthesizing of t-$ZrO_2$. Three phases of study were conducted in the quest to explore the polymer precursor method. The preliminary first phase was to study cooling process after calcinations. In the second phase the effect of the amount of polymer precursor was investigated. The third phase was a study on the dopants concentration effect and also the temperature stability of the doped powders. A soft-combustion method was conducted to compare with the polymer precursor decomposition synthesizing route in term of calcinations temperature as well as the properties of the samples produced. Study on solution

preparation, amount of precursors, calcinations, pelletization, sintering and optical bandgap were explored in both type experiments.

Characterization methods and equipments such as density measurement, surface area determination, X-Ray diffraction (XRD), scanning electron microscopy (SEM), transmission electron microscopy (TEM), differential thermal analysis (DTA) and UV-Visible Spectrometer were employed.

# CHAPTER 2
# LITERATURE REVIEW

## 2.1 Introduction

Zirconium dioxide ($ZrO_2$), also known as zirconia is a well studied material and has now been used in many applications. It has unique physical properties such as low thermal conductivity, high melting temperature, high hardness, low coefficient of friction, chemical inertness, low wear resistance and good ionic conductivity. Zirconia has been seen as one of the most promising ceramics for functional and structural materials [Tang et al., 2004]. The uses of zirconia in wide variety of technical applications make this compound an interesting subject for research works. For example, at the present time $ZrO_2$ has been developed to be used in wear resistant and refractories applications such as piston caps, extrusion dies and machinery wear parts as well as a solid electrolyte in furnace element, fuel cells and oxygen sensors [Amelinck et al., 1997].

Apart from its excellent applications as hard coatings and refractories ceramic components, $ZrO_2$ has been long known to be an ionic conductor. It has been reported that $ZrO_2$ has been used as electrolyte in Solid Oxide Fuel Cells (SOFC) and as oxygen sensors [Capel et al., 2002]. Nevertheless the electronic conductivity of $ZrO_2$ has remained a subject which requires further studies.

## 2.2 Polymorph

Zirconia exists in three polymorphs, i.e. monoclinic (m), tetragonal (t) and cubic (c). Below ~1170ºC zirconia occurs in the monoclinic terms, between ~1170ºC-2370ºC zirconia has tetragonal crystal structure, and above 2370ºC to the melting point of $ZrO_2$ (2680ºC), zirconia is in cubic structure [Stefanc et al., 1999-b].

c-$ZrO_2$ has fluorite structure, with each Zr ion having eight-fold coordination to the oxygen atoms, the Zr atoms form a fcc lattice and the oxygen atoms occupy the tetrahedral interstitial sites associated with the fcc lattice. Arranged in two equal tetrahedral around Zr, consequently, oxygen and zirconium are tetrahedrally and octahedrally coordinated respectively, and the unit cell contains one zirconium and two oxygen atoms. The cubic structure is fully determined by the single lattice constant, ***a*** [Munoz et al., 2006].

By displacing opposite pairs of oxygen atoms alternatively up and down along the z direction, t-$ZrO_2$ can be considered as a slightly distorted cubic structure. This doubles the primitive cell from one to two formula units, that is, from three to six atoms, and introduces a tetragonal strain. The structure can be specified by the two lattice parameters ***a*** and ***c***. In the tetragonal form the Zr ions are again eight-fold coordinated to O, with four oxygen neighbours arranged in a flattened tetrahedron at a short Zr-O distance, 2.065 Å, and the rest in an elongated tetrahedron rotated 90° at a distance of 2.455 Å from Zr [Munoz et al., 2006].

m-$ZrO_2$ formed by further distorting the tetragonal structure, with the lattice vectors no longer at right angles. It has a lower symmetry and a more complex geometric structure, with a 12-atom primitive cell. In m-$ZrO_2$, the Zr ions have seven-fold coordination to oxygen, and there are two non-equivalent oxygen sites: three-fold $O_I$ and four-fold $O_{II}$ (figure 2.1). The disposition of $O_{II}$ atoms is nearly tetrahedral, one angle (134.5°) in the structure differing significantly from the tetrahedral value (109.5°). Therefore, the arrangement of the oxygen atoms is not planar. A buckling occurs in the $O_{II}$ plane and the distribution of the $O_I$ atoms is quite irregular. There is a large dispersion of interatomic Zr-O distance, with average values of 2.07Å and 2.21 Å for Zr-$O_I$ and Zr-$O_{II}$, respectively [Munoz et al., 2006]. Figure 2.1 shows the atomic structure and Zr to O coordination units of zirconia polymorph.

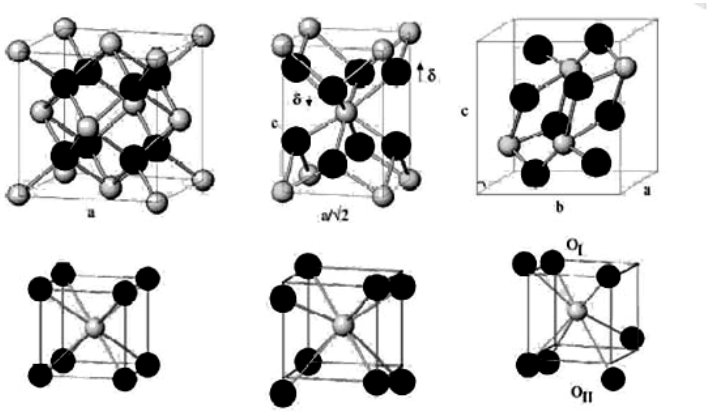


Figure 2.1: Atomic structure (top) and Zr to O coordination units (bottom) for the three low pressure polymorphs of $ZrO_2$: cubic (left), tetragonal (middle) and monoclinic (right). Large dark circles denote O atoms, small light circles, Zr [Munoz et al., 2006]

Table 2.1 shows some physical properties of zirconia polymorph.

Table 2.1: Physical properties of zirconia polymorph.

| Property | m-$ZrO_2$ | t-$ZrO_2$ | c-$ZrO_2$ | Reference |
|---|---|---|---|---|
| Bulk Density ($g/cm^3$) | 5.6 | 6.1 | 6.27 | Rudolph, 2004 |
| Band Gap (eV) | 5.83 | 5.78 | 6.1 | French et al., 1994 |
| Thermal expansion coefficient 0-1000°C ($x10^{-6}K^{-1}$) | - | 10.6 | - | Green et al., 1989 |
| Thermal expansion coefficient 0-1200°C ($x10^{-6}K^{-1}$) | 6.5 | - | 10.5 | American Elements Co (2007), Online |
| Lattice Parameters (nm) | a = 0.51507<br>b = 0.52031<br>c = 0.53154 | a = 0.50950<br>c = 0.51800 | - | Green et al., 1989 |
| Lattice Parameters (nm) | - | - | a = 0.50800 | Marshall et al., 1989 |

## 2.3 Phase Transformation

As reported, zirconia has three polymorphs; cubic, tetragonal and monoclinic. At room temperature, the monoclinic structure is the stable phase. Upon cooling from melting point, zirconia shows two kinds of solid-solid phase transformation, namely, cubic to tetragonal (c-t) [Yoshimura, 1988] and tetragonal to monoclinic (t-m) [Subbarao et al., 1974].

### 2.3.1 Cubic-Tetragonal

The cubic to tetragonal phase transformation in $ZrO_2$ ceramics, is similar to transformations in steels, and may be divided into two steps: the lattice rearrangement and the adjustment of chemical composition toward the equilibrium state [Zhou et al, 1991]. The lattice rearrangement from cubic to tetragonal structure requires the displacement of oxygen ions in order to increase the parameter of the c-axis and decrease the parameters of *a* and *b* axis. The appearance of tetragonality corresponds to the appearance of (112) reflections which are forbidden for the cubic phase. In this case a tweed structure forms throughout the specimen and the visible contrast in dark images taken by three (112) reflections is in fact a strain-type contrast induced by the uniformly distributed nuclei of the t-phase. In this case the chemical composition did not changed and remained just as the initial cubic phase [Zhou et al, 1991].

### 2.3.2 Tetragonal-Monoclinic

The t-m transformation occurs with a volume expansion and a shear distortion parallel to the basal plane of t-$ZrO_2$. These two characteristic can be used to increase both the strength and the toughness of zirconia. In fact, $ZrO_2$-based ceramic exhibits various outstanding properties that are closely related to the t-m phase transformation; for example, the volume change and the shear strain developed by the t-m transformation of metastable tetragonal particles act against the opening of a crack, and therefore increase the resistance of the ceramic to crack propagation. This mechanism significantly extends the reliability and lifetime of $ZrO_2$ derived materials and leads to the high fracture toughness of tetragonal zirconia [Garvie et al., 1975].

By using high temperature X-Ray Diffraction (XRD), Ruff and Ebert (1929) found the t-m transformation for the first time. Since then there were a lot of research

done using various technique, such as XRD, Different Thermal Analysis (DTA), morphology study and also electrical resistance [Subbarao, 1981].

Phase transformation from tetragonal to monoclinic is not isotropic. Lattice parameter *a* and *c* shows significant changes, but *b* value has a negligible changes [Patil and Subbarao, 1969]. Figure 2.2 shows the lattice parameters changes during transformation.

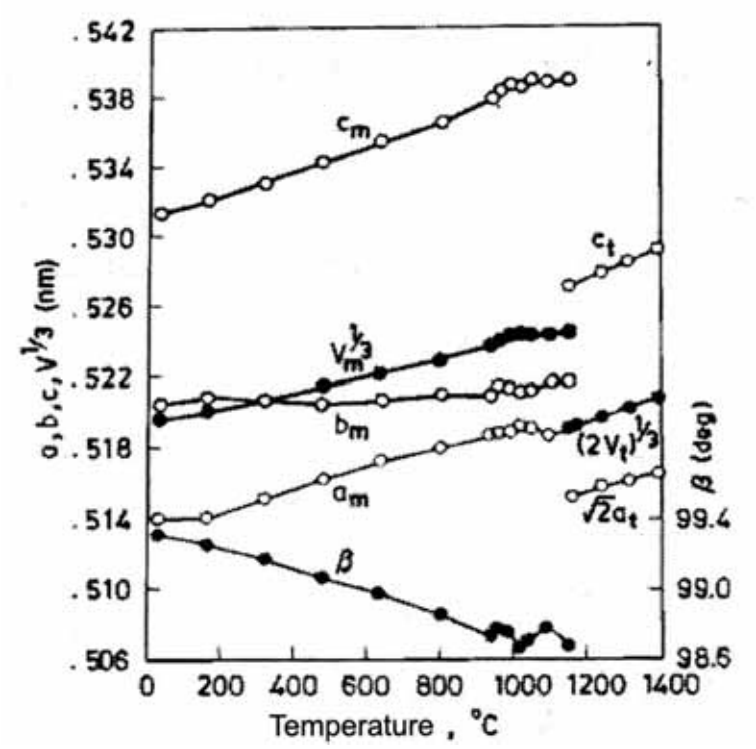


Figure 2.2: Lattice parameters changes during t-m transformation [Patil and Subbarao, 1969]. Where $a_m$ is "a" axis value of monoclinic phase, $b_m$ is "b" axis value of monoclinic phase, $c_m$ is "c" axis value of monoclinic phase, $c_t$ is "c" axis value for tetragonal phase, V is volume of the zirconia crystal structure and $\beta$ is angle between "a" and "c" axis

Tetragonal-monoclinic transformation shows large thermal hysterysis (Figure 2.3). The transformation to monoclinic during cooling process occurs between ~1000°C to ~650°C, whereby below this temperature all tetragonal would transform to

monoclinic. On the other hand, during heating process the transformation start at ~820°C and above ~1170°C full 100% tetragonal will form [Maiti et al., 1972].

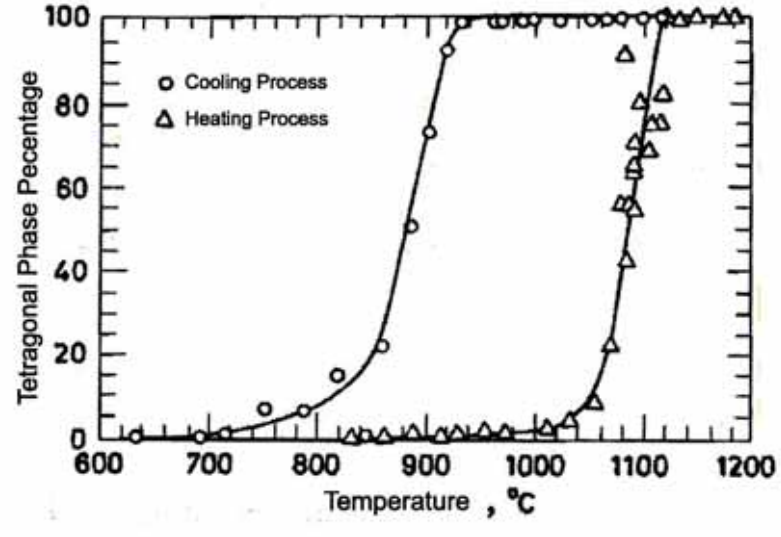


Figure 2.3: Tetragonal phase percentage during heating and cooling process [Maiti et al., 1972]

Morphology study by using Scanning Electron Microscope (SEM) (Figure 2.4) showed “needle like” structure of the zirconia after the t-m phase transformation. This structure had formed due to the diffusionless atomic movement [Bansal and Heuer, 1972 and 1974]. The t-m transformation is accompanied by a directional 5% increase in volume. Because the transformed particle is constrained by the matrix it cannot undergo its full macroscopic shape change. Nonetheless, the strain from the transformation must be accommodated in the monoclinic and surrounding grains. This has led to the suggestion that deformation twinning occurs to relieve the transformation stresses [Lee and Rainforth, 1994]. Evans et al. (1981) have shown that for this case most of the lattice strain is then confined to the matrix/monoclinic interface, and therefore there is no long range strain field associated with the transformation of a constrained particle. However, the lattice strain can clearly be large and therefore lead to micro-cracking either within the monoclinic particle and/or at the interface.

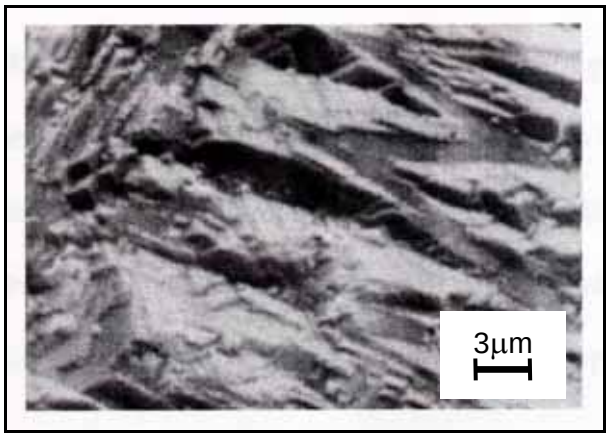


Figure 2.4: SEM micrograph of “needle like” structure of zirconia [Bansal and Heuer, 1972 and 1974]

## 2.4 Stabilization

Zirconia stabilization mechanism could be affected by several factors, some of which are influence by lattice defects, influence of particle size and influence of water vapor.

### 2.4.1 Influence of Lattice Defects

The effect of lattice defects on the stabilization of a metastable t-$ZrO_2$ was investigated by Torralvo et al.(1984) and Osendi et al.(1985). The studies investigated the formation of metastable t-$ZrO_2$ by the thermal decomposition of amorphous $ZrO_2$ precursor or zirconyl acetate, and they suggested that, nucleation of t-$ZrO_2$ was favored by creation of anionic vacancies with trapped electrons.

Doping with suitable aliovalent cations stabilizes c- and t-$ZrO_2$ at room temperature and gives rise to their functional properties. Oxide doping with MgO, CaO, CeO and especially $Y_2O_3$—due to its large solid solubility range in zirconia—is employed to partially or completely stabilize tetragonal and cubic structures. Reports showed Partially Stabilized Zirconia (PSZ), was obtained with Y content of about 2–7 mol% [Ray et al., 2000], while Fully Stabilized Zirconia (FSZ), requires Y content above 8 mol%, the typical doping being 14 mol% [Roxana et al., 2003]. Oxide doping not only

modifies the $ZrO_2$ structure, but also its vacancy concentration. This is because a large number of oxygen vacancies are introduced when, for example, divalent ($Mg^{2+}$) or trivalent ($Y^{3+}$) ions are incorporated into the zirconia structure for the purpose of phase stabilization. The large number of O vacancies leads to a high ionic conductivity, making the stabilized forms of zirconia one of the most useful electroceramics. In fact, PSZ and FSZ present important advantages, and they are used instead of pure $ZrO_2$ for most applications [Munoz et al., 2006]. FSZ and PSZ will be discussed in depth in the subsequent headings.

### 2.4.2 Influence of particle size

Reducing the crystal size to a few nanometers is another approach for stabilizing the high temperature phases at room temperature [Garvie, 1965; Garvie, 1985]. While m-$ZrO_2$ is the thermodynamically stable polymorph at room temperature in all system, t-$ZrO_2$ can be retained at room temperature provided that the particle size is below some critical value [Lee and Rainforth, 1994]. Above this critical size, spontaneous transformation will occur on cooling from the sintering temperature. Particles very much smaller than the critical size are resistant to transformation from propagating crack.

Chraska et al. (2000) found that any coarsening above a certain critical size results in particle transformation to the monoclinic phase. The critical size, up to which the tetragonal phase is stable, is around 18 nm in diameter (9 nm radius). Various explanations have been proposed for the observed stabilization of high temperature tetragonal phase in nanocrystalline zirconia particles at room temperature and controversies still exist in the elucidation of the mechanism of the t-phase stability. Garvie and Goss (1986) proposed that the lower surface energy of the t-$ZrO_2$ was the cause for this phase to be present in nanocrystalline form at or below room temperature. They predicted that particles below about 10 nm in diameter are stabilized

in the tetragonal form, and those that are above this critical particle size are subject to the t-m transformation.

Srinivasan et al. (1990) argued against the concept proposed Garvie and Goss (1986) (stabilization due to lower surface energy of the t phase) as they found monoclinic particles with much smaller diameters. They suggested that anionic oxygen vacancies present on the surface control the t-m phase transformation on cooling, and that oxygen adsorption triggers this phase transformation.

### 2.4.3 Influence of water vapor

Murase and Kato (1979 and 1983) examined the transformation of tetragonal $ZrO_2$ by ball-milling at different atmospheres. The results obtained indicated the important role of water adsorption on the surface of particles for the t-m transition of milled samples. The authors concluded that water vapor markedly accelerated crystallite growth of both m- and t-$ZrO_2$ and facilitated the t-m transformation.

### 2.4.4 Partially Stabilized Zirconia (PSZ)

Partially stabilized Zirconia is a mixture of zirconia polymorphs. PSZ formed because insufficient cubic phase-forming oxide added to the $ZrO_2$. A smaller addition of stabilizer to the pure zirconia will bring its structure into a tetragonal phase at a temperature higher than 1,000°C and a mixture of cubic phase and monoclinic (or tetragonal)-phase at a lower temperature [Stubican and Hellmann, 1981). Usually such PSZ consists of larger than 8 mol% (2.77 wt%) of MgO, 8 mol% (3.81 wt%) of CaO, or 3-4 mol% (5.4-7.1 wt%) of $Y_2O_3$ [Jaeger and Nickell, 1971].

PSZ is a transformation-toughened material. Micro-crack and induced stress may be two explainations for the toughening in partially stabilized zirconia. The micro-crack explaination depends upon difference in the thermal expansion between the

cubic phase particle and monoclinic (or tetragonal)-phase particles in the PSZ [Green et al., 1973 and 1974]. The difference in coefficient of thermal expansion between monoclinic and cubic phase creates micro-cracks that dissipate the energy of propagating cracks. The cubic matrix provides a compressive force that maintains the tetragonal phase. Stress energies from propagating cracks cause the transition from the metastable tetragonal to the stable m-$ZrO_2$. The energy used by this transformation is sufficient to slow or stop the propagation of the cracks.

### 2.4.5 Fully Stabilized Zirconia (FSZ)

FSZ is 100% cubic $ZrO_2$. The addition of more than 16 mol% of CaO (7.9 wt%) [Saha and Pramanik, 1995], 16 mol% MgO (5.86 wt%) [Porter and Heur, 1997], or 8 mol% of $Y_2O_3$ (13.75 wt%) [Roxana et al., 2003], into zirconia structure will form 100% c-$ZrO_2$ or is termed FSZ. Its structure becomes cubic solid solution, which has no phase transformation from room temperature up to 2,500 °C.

### 2.4.6 Defects

By the addition of aliovalent oxides into the zirconia, the high temperature cubic and tetragonal phases are partially or totally stabilized at room temperature. When divalent or trivalent ions such as Mg, Ca or Y are incorporated into the zirconia matrix, the dopant cations substitute Zr atoms and therefore introducing oxygen vacancies into the anion sites to maintain electrical neutrality. Thus, PSZ and FSZ not only contain the stabilizing dopants, but also a significant amount of oxygen vacancies. Their presence gives rise to the large ionic conductivity of oxide-stabilized zirconia. The long range transport of oxygen ions occurs by hopping between anion sites via the vacancies. In addition, $ZrO_2$ sintering methods performed in a reducing atmosphere result in the production of another kind of oxygen vacancies, the so-called neutral or thermodynamic vacancies [Munoz et al., 2006].

It has been demonstrated that thermodynamic vacancies also exert a considerable stabilizing effect on the tetragonal $ZrO_2$ phase [Zu and Yan, 1997], The symmetry of the lattice is broken by dopants and the appearance of oxygen vacancies, giving rise not only to structural modifications associated with the phase transformation, but also to change in the electronic properties of the ceramic [Munoz et al., 2006].

Capel et al. (2002) discovered that the incorporation of titania ($TiO_2$) into ceria-stabilized tetragonal zirconia decreases the ionic conductivity in air of the formed ternary t-$ZrO_2$ solid solutions with increasing titania content. It is believed that such a conductivity decrease is due to the formation of oxygen vacancy-cation associations (Ti–$V_{ö}$) with low vacancy diffusion dynamic resulting, thus, in a decrease in the global concentration of moving oxygen vacancies. Interestingly, for $TiO_2$-doped Zirconia, they found that with decreasing oxygen partial pressures a strong departure from stoichiometry with the reduction of $Ti^{4+}$ to $Ti^{3+}$ seems to take place. This indicates that the conduction process is controlled by the $Ce'_{Zr}$ and $Ti'_{Zr}$ defect concentrations. Assuming that the electrons are located on cerium and titanium sites, the electrical conduction occurs by hopping of the electrons between $Ce^{4+}$ and $Ce^{3+}$ and $Ti^{4+}$ and $Ti^{3+}$ via a small polaron hopping mechanism. Botta et al. (1999) also found that the incorporation of Fe(III), acting as an electron or hole trapping center in zirconia, managed to produce t-$ZrO_2$ with energy bandgap in ranges of 2.2-2.4 eV.

When a trivalent oxide, e.g. $Y_2O_3$, is added to $ZrO_2$ as stabilizer, certain amount of lattice defects, e.g. oxygen vacancies $V_{Ö}$ and negatively-charged solutes $Y'_{Zr}$ are produced in the $ZrO_2$ lattice. The conductivity of stabilized-$ZrO_2$ is determined by its defect structure, chiefly $V_{Ö}$, $Y'_{Zr}$ and the defect associates between them in the case of $Y_2O_3$ stabilized $ZrO_2$ (YSZ) [Guo and Wang, 1997].

The lattice defect in YSZ is the grain boundaries and point defects. The major point defects in YSZ are $Y'_{Zr}$. and $V_{Ö}$. However, $V_{Ö}$ will repulse positrons due to its positive charge. Because of coulombic interaction between the charged defects, some defect associates may be formed. It has been proved that ($Y'_{Zr}V_{Ö}$) is the dominant defect associate in dilute $Y_2O_3$ and $ZrO_2$ solution; in $ZrO_2$ with high $Y_2O_3$ concentration, the formation of ($Y'_{Zr}V_{Ö}Y'_{Zr}$) is possible [Subbarao and Maiti, 1984].

The defect reactions can be summarized as follows [Guo and Wang, 1997]:

$$Y_2O_3 \rightarrow 2Y'_{Zr} + V_{Ö} + 3O_O^x \qquad (2.1)$$

$$Y'_{Zr} + V_{Ö} \rightarrow (Y'_{Zr}V_{Ö}) \qquad (2.2)$$

$$(Y'_{Zr}V_{Ö}) + Y'_{Zr} \rightarrow (Y'_{Zr}V_{Ö}Y'_{Zr})^x \qquad (2.3)$$

Pentavalent oxides are positively charged, and opposite to the stabilizers. When dissolved in the $ZrO_2$ lattice, the addition of pentavalent oxides in the stabilized-$ZrO_2$ will definitely affect the original defect structure, thus influencing the properties of the stabilized-$ZrO_2$. Tantalum oxide ($Ta_2O_5$) has been found to affect the phase stability and the electrical properties of $ZrO_2$, while $Nb_2O_5$ has also been found to dramatically change the grain boundary conductivity [Kim and Tien, 1991; Gou, 1997].

$Nb_2O_5$ can only be substitutionally dissolved in $ZrO_2$, because it is obviously impossible to be interstitially dissolved when considering the relatively large radius of $Nb^{5+}$ with respect to the interstices in the $ZrO_2$ lattice. The most probable dissolving mechanism of $Nb_2O_5$ in $ZrO_2$ is [Guo and Wang, 1997]:

$$Nb_2O_5 \rightarrow 2Nb_{Zr^{\cdot}} + 2e + 4O_O^x + 1/2O_2 \qquad (2.4)$$

The addition of $Nb_2O_5$ does not introduce new positron-sensitive defect into YSZ, but introduces 2 mol% free electrons for every molar fraction of $Nb_2O_5$. The free electrons thus produced may annihilate $V_{\ddot{O}}$ by the following defect reactions [Guo and Wang, 1997]:

$$2e + V_{\ddot{O}} \rightarrow (2eV_{\ddot{O}})^{x} \qquad (2.5)$$

or

$$2e + V_{\ddot{O}} \rightarrow null \qquad (2.6)$$

so the $V_{\ddot{O}}$ concentration in the specimens with $Nb_2O_5$ additions is reduced. If the annihilation of $V_{\ddot{O}}$ is accomplished by the formation of color centers $(2e\ V_{\ddot{O}})^{x}$ (equation 2.5), which will induce the color of brown or gray in the specimens then the color of the specimens with $Nb_2O_5$ additions should not be white [Guo et al.,1996]. However, if there are no changes of color, the annihilation of $V_{\ddot{O}}$ should be accomplished according to equation (2.6) [Guo and Wang, 1997].

The addition of $Ta_2O_5$ or $Nb_2O_5$ to YSZ does not change the conduction mechanism [Guo, 1997-a], but $Nb^{5+}$ ion on the $Zr^{4+}$ site implies a net effective charge of +1, which repels $V_{\ddot{O}}$. This increases the difficulty of the $V_{\ddot{O}}$ movement in the YSZ lattice, so the mobility decreases, which also increases the ionic bulk resistivity.

The annihilation of $V_{\ddot{O}}$ can also increase $(Y'_{Zr}\ V_{\ddot{O}}\ Y'_{Zr})^{x}$. The mechanism can be explained by the compensation effect between the acceptor ($Y_2O_3$) and the donor ($Nb_2O_5$) [Kountouros and Petzow, 1993]. According to equation (2.2), the concentration of $(Y'_{Zr}\ V_{\ddot{O}})$ is also reduced due to the reduced $V_{\ddot{O}}$ concentration. The reduced $[(Y'_{Zr}\ V_{\ddot{O}})]$ increases the $[Y'_{Zr}]$ in the reaction (2.3), this may increase the concentration of $(Y'_{Zr}\ V_{\ddot{O}}\ Y'_{Zr})^{x}$, according to equation (2.3) [Guo and Wang, 1997].

In addition, there may be another possible defect reaction involved in the $Nb_2O_5$ additions [Guo and Wang, 1997]. At high $Nb_2O_5$ concentration, because of the expected repulsive force between $Nb_{Zr}^{\cdot}$ and $V_{\ddot{O}}$, the introduction of $Nb_{Zr}^{\cdot}$ into YSZ may suppress the formation of the defect associates, even split the already formed defect associates, i.e. two defect reactions defined as follows may occur:

$$(Y_{Zr}^{'}V_{\ddot{O}}Y_{Zr}^{'})^{x} \overset{Nb_{Zr}^{\cdot}}{\rightarrow} (Y_{Zr}^{'}V_{\ddot{O}}) + Y_{Zr}^{'} \qquad (2.7)$$

$$(Y_{Zr}^{'}V_{\ddot{O}}) \overset{Nb_{Zr}^{\cdot}}{\rightarrow} Y_{Zr}^{'} + V_{\ddot{O}} \qquad (2.8)$$

which will increase the concentration of mobile $V_{\ddot{O}}$. This surely decreases the concentration of the only positron-sensitive defect associate in YSZ: $(Y'_{Zr}\ V_{\ddot{O}}\ Y'_{Zr})^{x}$. However, this certainly will also decrease the bulk resistivities [Choudhary and Subbarao, 1979; Guo and Wang, 1997].

At present, there is no stabilized $ZrO_2$ structure for which the origin and strength of defect interactions can be completely understood. Even for the most studied case, yttria stabilized zirconia (YSZ), the experimental results support different defect configurations. Some of research suggest that oxygen vacancies are bonded to the dopant Y [Steele and Fender, 1974; Li and Hafskjold, 1995], others claim host Zr–vacancy bonds [Catlow et al., 1986; Goff et al., 1999]. The strength of the vacancy–ion bonds is also a matter of discussion.

### 2.4.7 Sintering Behaviour of $Y_2O_3$-$Nb_2O_5$ doped-Zirconia

In the $ZrO_2$-$Y_2O_3$-$Nb_2O_5$ system, as the $Nb_2O_5$ content increased up to 1.5 mol%, the rate of low-temperature degradation (LTD) was reported to rise due to the increase in the c/a axial ratio (tetragonality) of the t-$ZrO_2$ solid solution. The measurements was done to the sample that prepared by ceramic processing

method which involves mixing, ball-milling, pressing and sintering at 1500°C for two hours [Guo, 1997-b]. This was associated with the internal strain, as a result of annihilation of oxygen vacancies introduced by $Y^{3+}$ [Kim et al., 1995; Kim et al., 1998]. On the other hand, having a composition of 90.24 mol% $ZrO_2$ ; 5.31 mol% $Y_2O_3$; 4.45 mol% $Nb_2O_5$ (5.31Y-TZP) that sintered at temperatures of 1500-1650°C with a heating rate of 6°C $min^{-1}$ up to 900°C and a heating rate of 3°C $min^{-1}$ up to the sintering temperature and then furnace cooled to room temperature, showed excellent phase stability and fracture toughness due to local Y-Nb dopant ordering in t-$ZrO_2$ into a scheelite-like arrangement, which resulted in a relief of the internal strain in the t-$ZrO_2$ lattice [Lee et al., 1998]. In the ordered structure, the smaller cation $Nb^{5+}$ adopts a four-fold coordination leaving eight-fold coordination to $Y^{3+}$, determined by the observation of X-ray absorption spectroscopy [Li et al., 1994].

The absence of LTD in TZP doped with certain $Nb_2O_5$ concentration indicates two types of t-$ZrO_2$ phases, i.e. a stable t-$ZrO_2$ in the system $ZrO_2$-$YNbO_4$ and a degradable t-$ZrO_2$ in the system $ZrO_2$-$Y_2O_3$, may coexist. However, the stable t-$ZrO_2$ phase would hamper the t-m phase transformation of the degradable t-phase. This was due to lattice relaxation of the degradable t-$ZrO_2$ is restrained significantly by the stable t-phase. The stable t-$ZrO_2$, which does not transform to m-$ZrO_2$ during low temperature aging, exists due to local Y-Nb ordering in the composition region with 14±15 mol% $YNbO_4$ in the $ZrO_2$-YNbO4 quasibinary system [Lee et al., 1998]. At 4.45 mol% $Nb_2O_5$, $Nb^{5+}$ necessary for the stability of t-$ZrO_2$ is dissipated by the proper substitution so that Y-Nb dopant ordering into a scheelite-like structure is achieved and the relaxation of the internal strain inherent in the t-lattice is accomplished. Beyond 4.6 mol% $Nb_2O_5$ , the fraction of m-$ZrO_2$ starts to increase again, implying that the addition of excess $Nb^{5+}$ into t-$ZrO_2$ increases the internal strain more significantly than TZPs doped with a small amount of $Nb_2O_5$ [Lee et al., 2001].

The composition region of t-$ZrO_2$ solid solutions in the system $ZrO_2$-$Y_2O_3$-$Nb_2O_5$ at 1500°C was determined and illustrated in Fig. 2.5. The t-$ZrO_2$ phase can be classified as either a degradable Tetragonal Zirconia Polycrystalline (TZP-Tss) or a stable TZP (NTss) under the ageing environment, depending on the composition. To produce stable TZP, 14-15 mol% $YNbO_4$ was needed in the quasibinary system of $ZrO_2$-$YNbO_4$.

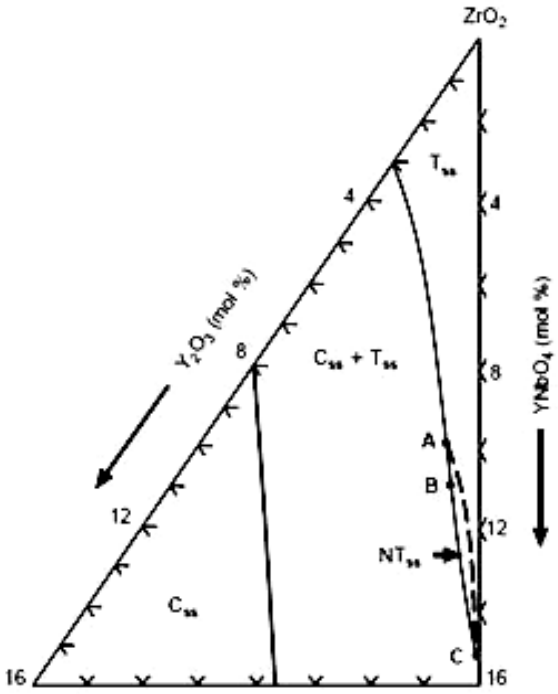


Figure 2.5: Part of the simplified ternary phase diagram for the system $Y_2O_3$-$Nb_2O_5$-$ZrO_2$ at 1500°C. Tss, Css and NTss are t-$ZrO_2$, cubic $ZrO_2$ and non-transformable t-$ZrO_2$ solid solution, respectively. A, B and C indicate the 90 mol% $ZrO_2$-5.5 mol% $Y_2O_3$-4.5 mol% $Nb_2O_5$, 89 mol% $ZrO_2$-6 mol% $Y_2O_3$-5 mol% $Nb_2O_5$ and 85 mol% $ZrO_2$-7.5 mol% $Y_2O_3$-7.5 mol% $Nb_2O_5$ compositions, respectively [Lee et al., 1998]

In a conclusion, the addition of $Nb_2O_5$ to bulk $Y_2O_3$-stabilized tetragonal $ZrO_2$ increases the transformability (t-m transformation temperature) of the resulting zirconia ceramics. The enhanced transformability is related to the alloying effect on the tetragonality (c/a—cell parameters ratio) of stabilized tetragonal $ZrO_2$. The increase in the tetragonality due to alloying is consistent with the increase in the

fracture toughness and the increase in the t-m transformation temperature. [Kim, 1990; Kim and Tien, 1991]

### 2.4.8 Electronic Structure

The electronic structure of zirconia can be roughly described as a valence band formed by the filled O 2p orbitals and a conduction band formed by the empty Zr 4d metal levels [Kralik et al., 1998]. The calculated electronic properties are in good agreement with the available experimental data, even though they do not describe properly the band gap and other excited-state properties. However, after including electron self-energy corrections, the structural and quasiparticle properties of the three $ZrO_2$ phases reach an improved level of agreement with experiments.

Band structures of the monoclinic, tetragonal and cubic phases are shown in Fig. 2.6. The valence bands (VBs) of the three phases are very similar. Starting from the lowest energies, the first contribution arises from the O 2s states and is centered around ~18 eV below the Fermi level ($E_F$) depending on the phase. The oxygen 2p band, completely filled by the transfer of Zr 4d electrons, is the occupied structure of highest energy. The maximum of the VB is located at the reciprocal point X in the cubic lattice and at $\Gamma$ in the monoclinic one, while in the tetragonal phase it comprises various points along the $\Gamma$ M and $\Gamma$ Z directions. The calculated VB O 2p width is around 5 eV for the monoclinic and tetragonal phases, and about 6 eV for c- $ZrO_2$. All phases present an indirect energy gap [Munoz et al., 2006].

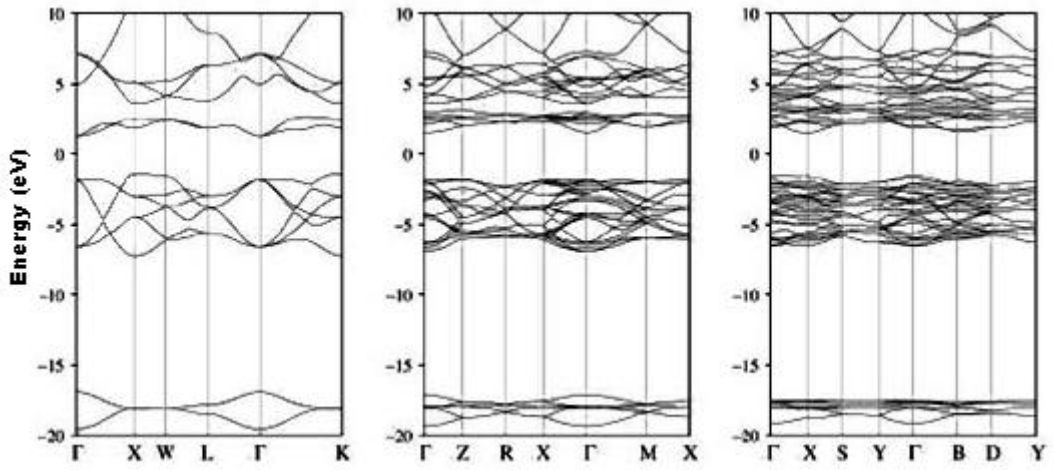


Fig. 2.6. Band structure of cubic (left), tetragonal (middle) and monoclinic (right) $ZrO_2$ along high symmetry directions. The energy zero is set at the Fermi level [Munoz et al., 2006]

## 2.5 Production of Nanocrystal Tetragonal Zirconia Powder

There is a growing need for nanosized mixed oxide ceramic powders for advanced technological applications. Often these advanced ceramic materials are tailormade to suit specific application [Das and Pramanik, 2000]. The prefix “nano” means one billionth. Nanoscience is the study of the fundamental principles of molecules and structures with at least one dimension roughly between 1 and 100 nanometers. These structures are known as nanostructures. Nanotechnology is the application of these nanostructures into useful nanoscale devices. Anything smaller than a nanometer in size is just a loose atom or small molecule floating in space. So at present, nanostructures are the smallest solid things it is possible to make. Additionally the nanoscale is unique because it is the size scale where the familiar properties of materials like conductivity, hardness, or melting point meet the more exotic properties of the atomic and molecular world such as wave-particle duality and quantum effects. At nanoscale, the most fundamental properties of materials and machines depend on their size in a way they don’t at any aother scale [Ratner and Ratner, 2003].